Rapid Communications

Possibility to produce ^{293,295,296}Og in the reactions ^{48}Ca + ^{249,250,251}Cf

X. J. Bao (包小军)*

Department of Physics, Collaborative Innovation Center for Quantum Effects, Key Laboratory of Low Dimensional Quantum Structures, Quantum Control of Ministry of Education, Hunan Normal University, Changsha 410081, People's Republic of China

(Received 10 March 2019; revised manuscript received 30 June 2019; published 23 July 2019)

The influence of polarization effects and temperature effects on the deformations of projectilelike and targetlike densities are taken into account consistently on the potential-energy surface. The evaporation residue cross sections for hot-fusion reactions are investigated within the dinuclear system model. The calculated results have reproduced well the experimental trend and absolute value of the maximum cross sections for 3*n* and 4*n* channels. The new isotopes of ^{293,295,296}Og were found to be as large as about 0.1–0.2 pb.

DOI: 10.1103/PhysRevC.100.011601

Producing superheavy nuclei (SHN) is one of the major aims of modern nuclear heavy-ion physics [1,2]. Many approaches have been used for the investigation of the synthesis mechanism of SHN [3–6]. Systematic calculations have been performed to describe the evaporation residue cross sections (ERCSs) with the Langevin dynamics model [7], the fusion-by-diffusion model [8], the dinuclear system (DNS) model [9], and shape evolution and tunneling [5]. No approach is currently predominant.

To describe the theoretically fusion mechanism, one must consider several important degrees of freedom [10]. The factors, such as the mass and charge asymmetries of projectile-target combinations [11,12], the distance between the nuclear centers [10,13,14], deformations and corresponding orientation effects [15–17], which influence the dynamics from the touching configuration to the compound nucleus and, thus, affect the fusion probability [18].

Two main reasons stimulated the theoretical study of the synthesis process of the superheavy nuclei. First, one needs to understand and shed light on the fusion mechanism of superheavy nuclei. Second, the favorable beam energy and the optimal projectile-target combination should be searched to produce new isotopes of superheavy nuclei [19].

The experiment discovered that one of the important factors is the effect of the nuclear orientation on the fusion probability [20,21]. From the theoretical point of view, the Coulomb barrier and depth of the pocket of the nucleus-nucleus potential are different for collisions of the deformed target or/and projectile nucleus with different orientations [22]. Therefore, the nucleus-nucleus interaction potential is the most important quantity not only in the capture cross sections, but also in the fusion probabilities.

In the dynamical evolution process, the dissipation kinetic energy of relative motion can provide a higher excitation energy, and at sufficiently high excitation energies, the individual shell structure of nuclei become the damping shell correction [23]. One has to consider how shell structure is reorganized with deformation and excitation energy [24–26]. Thus, for practical calculations, a theoretical estimate of the thermal damping shell correction is needed, which can allow a better understanding of behaviors of the dynamical potential-energy surface shedding some interesting light on the reaction mechanism. However, not very much work involves the shell correction energy employed in the fusion process being nuclear temperature dependent [27,28].

I would like to elucidate the influence of orientation effects and temperature effects on the ERCS in the DNS model. In addition, this Rapid Communication is to give predictions for the experiment being under way at the Oak Ridge National Laboratory in which a target consisting of a mixture of $^{249-251}$Cf isotopes was bombarded with the ^{48}Ca beam in order to synthesize new isotopes of the element $Z = 118$ [19]. The theoretical prediction results are helpful for the interpretation of experimental results.

The ERCS in heavy-ion fusion reactions is calculated as the summation over all partial waves J [29],

$$\sigma_{\rm ER}(E_{\rm c.m.}) = \sum_J \sigma_{\rm cap}(E_{\rm c.m.}, J) P_{CN}(E_{\rm c.m.}, J) W_{\rm sur}(E_{\rm c.m.}, J), \tag{1}$$

where $E_{\rm c.m.}$ is the incident energy in the center-of-mass frame. The capture cross section $\sigma_{\rm cap}(E_{\rm c.m.}, J)$ for each partial-wave J at a given center-of-mass energy $E_{\rm c.m.}$ can be written as [30]

$$\sigma_{\rm cap}(E_{\rm c.m.}, J) = \frac{\pi\hbar^2}{2\mu E_{\rm c.m.}} \int_0^{\pi/2} \sin\theta_1 d\theta_1 \times \int_0^{\pi/2} (2J+1) T(E_{\rm c.m.}, J, \theta_1, \theta_2) \sin\theta_2 d\theta_2, \tag{2}$$

where $T(E_{\rm c.m.}, J, \theta_1, \theta_2)$ denotes the penetration probability [30]. The influence orientation effects on the capture cross section have been included through the dependence of the nucleus-nucleus potential on the orientation angles. The Coulomb and nuclear interactions are addressed in detail in Refs. [30,31].

*baoxiaojun@hunnu.edu.cn

The $P_{CN}(E_{\rm c.m.}, J)$ in Eq. (1) is the probability that the system evolves from a touching configuration to the formation of compound nucleus. The time evolution of the probability distribution function $P(Z_1, N_1, \beta_{12}, \beta_{22}, \varepsilon_1, t)$ can be obtained by solving four variable master equations in the corresponding potential-energy surface [32], which is addressed in detail in Ref. [33].

According to statistical mechanics, the character that the shape of the nucleus tends to be spherical at high excitation energy (excitation effects) should be included. Meanwhile, both nuclei in the DNS should be gradually deformed due to strong nuclear and Coulomb interactions between them (polarization effects). One has to regard that the deformations of the DNS deviate from their values in the ground states. In order to consider consistently the influence of excitation effects and polarization effects on the deformations of projectilelike and targetlike densities, the β_{12} and β_{22} are considered as two discrete variables. Thus, the more real potential-energy surface where the DNS evolves with the orientation and deformation effects are modified to

$$\begin{aligned} &U(N_1, Z_1, N_2, Z_2, R, \beta_{i2}, \beta_{i4}, \theta_1, \theta_2) \\ &= U_C(Z_1, Z_2, R, \beta_{i2}, \beta_{i4}, \theta_1, \theta_2) \\ &\quad + U_N(N_1, Z_1, N_2, Z_2, R, \beta_{i2}, \beta_{i4}, \theta_1, \theta_2) \\ &\quad + B^1_{LD}(N_1, Z_1, \varepsilon_1) \prod_{k=2 \text{ and } 4} \left(1 + b_k \beta_k^2\right) \\ &\quad + E^1_{\rm shell}(N_1, Z_1, \beta) \exp(-\gamma_D \varepsilon_1) \\ &\quad + B^2_{LD}(N_2, Z_2, \varepsilon_2) \prod_{k=2 \text{ and } 4} \left(1 + b_k \beta_k^2\right) \\ &\quad + E^2_{\rm shell}(N_2, Z_2, \beta) \exp(-\gamma_D \varepsilon_2) - B_{CN}. \end{aligned} \tag{3}$$

The Coulomb interaction $U_C(Z_1, Z_2, R, \beta_{i2}, \beta_{i4}, \theta_1, \theta_2)$ can be calculated by Wong's formula [30]. The nuclear potential $U_N(N_1, Z_1, N_2, Z_2, R, \beta_{i2}, \beta_{i4}, \theta_1, \theta_2)$ is to fold a nucleon-nucleon interaction with the projectile and target densities, which is addressed in detail in Ref. [31]. The nuclear density distribution functions ρ_1 and ρ_2 are two-parameter Woods-Saxon types,

$$\rho_1(\mathbf{r}) = \frac{\rho_{00}}{1 + \exp\{[\mathbf{r} - R_1(\alpha_1)]/a_{\rho 1}\}}, \tag{4}$$

and

$$\rho_2(\mathbf{r}) = \frac{\rho_{00}}{1 + \exp\{[|\mathbf{r} - \mathbf{R}| - R_2(\alpha_2)]/a_{\rho 2}\}}. \tag{5}$$

The parameters $a_{\rho 1}(a = 0.54)$ and $a_{\rho 2}(a = 0.54)$ represent the diffuseness of the two nuclei, respectively.

The deformation-dependent binding energies $B^i_{LD}(N_i, Z_i, \varepsilon_i) \prod_{k\geqslant 2}(1 + b_k \beta_k^2) + E^i_{\rm shell}(N_i, Z_i, \beta) \exp(-\gamma_D \varepsilon_i)(i = 1, 2)$ are calculated by the macroscopic-microscopic model [34], which is addressed in detail in Refs. [33,34]. The energy of a nucleus with respect to the axial deformations is calculated, and only axially deformed cases β_{i2} and β_{i4} are considered in the macroscopic-microscopic model [34]. The binding energy and the deformation of the ground state obtained with this method are very close to the results in Möller's table [35]. In the present Rapid Communication, the notation $\beta_k \equiv \beta_{i2}$ and β_{i4}, which gives the total energies of the ith nucleus with the values of β_{i2} and β_{i4}. β_{i2} $(i = 1, 2)$ denotes quadrupole deformations of fragments, and they are considered as two discrete variables. The ground-state value of hexadecapole deformations β_{i4} $(i = 1, 2)$ remains unchanged.

ε_i is allocated from the local excitation energy of the DNS, according to the mass number A_i. It is well known that the shell damping is due to excitation energy. There are two different approaches for the shell damping taking into account the shell correction dependent on excitation energy [36]. The first approach is that the modification of the Fermi-gas level-density parameter suggested by Ignatyuk *et al.* [37] and the latter part will give a detailed calculation in Eq. (10) for survival probability. Another approach assumes that the potential energy should be temperature dependent itself [25,26]. The latter approach is adopted for temperature effects on the potential-energy surface. The damping factor γ_D means the speed of washing out the shell correction against the excitation energy (temperature effects). In principle, the dependence of the γ_D value on excitation energy changes rapidly with proton and neutron numbers [38,39]. In the present Rapid Communication, $\gamma_D = 0.048\,84$ MeV is used from Ref. [40], which is the average value between 1/10 and 1/30 MeV [38,41].

The local excitation energy ε is defined as [42]

$$\begin{aligned} \varepsilon = E_x - \big[&U(N_1, Z_1, N_2, Z_2, R, \beta_{i2}, \beta_{i4}, \theta_1, \theta_2) \\ &- U(N_P, Z_P, N_T, Z_T, R, \beta^0_{i2}, \beta_{i4}, \theta_1, \theta_2)\big], \end{aligned} \tag{6}$$

where the first term denotes that the dissipation energy E_x of the composite system is converted from the relative kinetic-energy loss [43]. The dissipation energy E_x is related to the minimum value of the interaction potential of the nucleus-nucleus and is determined by the parametrization method of the classical deflection function.

Finally, the distribution function $P(Z_1, N_1, \beta_{12}, \beta_{22}, \varepsilon_1, t)$ is calculated by solving four variable partial differential equations numerically. The fusion probability is given by

$$\begin{aligned} P_{CN}(E_{\rm c.m.}, J) = &\sum_{Z_1=1}^{Z_{\rm BG}} \sum_{N_1=1}^{N_{\rm BG}} \int_0^\infty \int_0^\infty \int_0^{\pi/2} \sin\,\theta_1 d\theta_1 \\ &\times \int_0^{\pi/2} P(Z_1, N_1, \beta_{12}, \beta_{22}, \theta_1, \theta_2, \tau_{\rm int}) \rho_1 \\ &\times (\beta_{12}) \rho_2(\beta_{22}) d\beta_{12} d\beta_{22} \sin\,\theta_2 d\theta_2. \end{aligned} \tag{7}$$

Here, $\tau_{\rm int}$ denotes interaction time in the dissipative process. $N_{\rm BG}$ and $Z_{\rm BG}$ are the Businaro-Gallone (BG) points.

The last term $W_{\rm sur}(E_{\rm c.m.}, J)$ in Eq. (1) is the survival probability of the formed compound nucleus, which can be estimated with a statistic model. The survival probability of the excited compound nucleus in the deexcitation process by means of the neutron evaporation in competition with fission is expressed as the following:

$$W_{\rm sur}(E^*_{CN}, x, J) = F(E^*_{CN}, x, J) \prod_{i=1}^{x} \left[\frac{\Gamma_n(E^*_i, J)}{\Gamma_n(E^*_i, J) + \Gamma_f(E^*_i, J)}\right]_i, \tag{8}$$

where, $F(E^*_{CN}, x, J)$ is the realization probability [44] of the xn channel at the excitation energy $E^*_{CN}(E_{\rm c.m.}+Q)$ of the compound nucleus with the angular momentum J and i is the index of evaporation step. Γ_n [45,46] and Γ_f [47] are the partial widths of neutron emission and fission.

The backshift Fermi-gas model at energies of the hot-fusion reaction of interest is used to determine the level density,

$$\rho(U,J)=\frac{(2J+1)\exp\left[2\sqrt{aU}-\frac{J(J+1)}{2\sigma^2}\right]}{24\sqrt{2}\sigma^3 a^{1/4}U^{5/4}}, \tag{9}$$

with $\sigma^2=\frac{\Theta_{\rm rigid}}{\hbar^2}\sqrt{\frac{U}{a}}$, $\Theta_{\rm rigid}=\frac{2}{5}m_uAR^2$, $U=E-\delta$. The back-shifts $\delta=-\Delta$ (odd-odd), 0 (odd-A), and Δ (even-even), respectively, are related to the neutron and proton paring gap $\Delta=1/2[\Delta_n(Z,N)+\Delta_p(Z,N)]$ which is employed from mass differences of neighboring nuclei [40]. The dependence of the level-density parameter a on the shell correction and the excitation energy was initially proposed

$$a(U,Z,N)=\tilde{a}(A)\left[1+E_{\rm sh}\frac{f(U)}{U}\right], \tag{10}$$

with $\tilde{a}(A)=\alpha A+\beta A^{2/3}$ and $f(U)=1-\exp(-\gamma_D U)$. It is worth noting that the differences between the corresponding level-density parameters are mainly related to different shell corrections and, thus, one should use these parameters at the same shell correction energies. In the present Rapid Communication, parameters $\alpha=0.1337$, $\beta=-0.065\,71$, and $\gamma_D=0.048\,84$ [40] determined by fitting to experimental level-density data with the help of the microscopic shell correction from FRDM95 [35] are adopted to calculate the level density used in the evaporation calculations.

Figures 1(a)–1(c) show the capture cross section $\sigma_{\rm cap}$ as a function of the incident energy in the center-of-mass frame. I compared calculations of the capture cross sections for the ^{48}Ca + ^{238}U, ^{48}Ca + ^{244}Pu, and ^{48}Ca + ^{248}Cm reactions with the measured cross sections. The average results are in good agreement with the experimental data [48] for the three reactions.

In order to illustrate the influence of the orientation effects on the ERCS, the calculated results with the different orientation angles are given in Figs. 1(d)–1(f). The black and the red lines denote the ERCRs of the 3n and the 4n channels, respectively. The solid lines represent the average results for different orientation angles. The experimental data [49] are reproduced well for the three reactions. Figures 1(d)–1(f) also show the ERCSs for tip-tip (0-0) and side-side ($\pi/2$-$\pi/2$) by the short dashed and the dashed lines, respectively. One can see that the 3n and 4n channels are mainly due to the side-side collision with ($\pi/2$-$\pi/2$). The result is consistent with the experimental conclusions in Refs. [20,21].

Now, I investigate how the orientation angles from different combinations influence the capture cross section and the fusion probability. The investigation is carried out for ^{48}Ca + ^{244}Pu based on the orientation angle combinations from three cases: 0-0 (tip-tip), $\pi/4$-$\pi/4$, and $\pi/2$-$\pi/2$ (side-side). Figure 2(a) shows the capture cross section $\sigma_{\rm cap}$ as a function of the excitation energy of the compound nucleus.

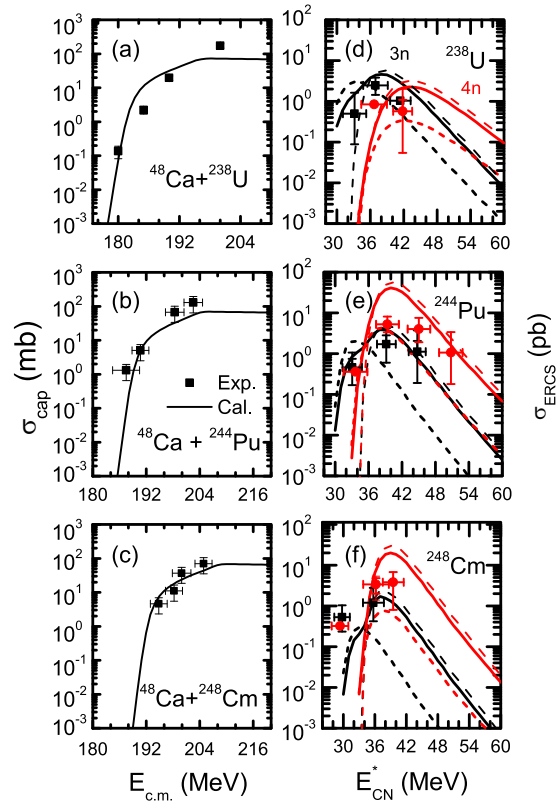

FIG. 1. The capture cross sections for ^{48}Ca + ^{238}U, ^{48}Ca + ^{244}Pu, and ^{48}Ca + ^{248}Cm reactions are calculated in the left panels. The experimental data are taken from Ref. [48]. The evaporation residue cross sections for the three systems as a function of the excitation energy in the right panels. The solid lines are obtained by taking an average over all the angles, and the short dashed and the dashed lines show the cross sections for the orientation angle of tip-tip and side-side, respectively. The experimental data are taken from Refs. [48,49].

In the lower excitation energy region $E^*_{CN}<40$ MeV, the capture cross sections for the tip-tip case are larger than those of the side-side and other combination cases because of the value of Coulomb barrier $V_{\rm CB}$ increases drastically with increasing the value of θ_2 [22]. When increasing excitation energy increases beyond 40 MeV, the capture cross sections almost tend to be all consistent.

The fusion probability P_{CN} from different orientation angles is shown in Fig. 2(b). The potential-energy surfaces for the three cases are shown in Fig. 2(c). In the present Rapid Communication, probabilities distribution in the left area of the BG point are assumed to contribute to the fusion probability. The probabilities distribution of the DNS configurations are governed by the dimension of single-particle states of projectilelike and targetlike nuclei and the mean transition probability between different states which depends on the local excitation energy. As shown in Eq. (6), the local excitation energy is determined by the dissipation energy and the relative potential-energy surface. In the tip-tip case, the high inner fusion barrier is not in favor of fusion, but the dissipation energy E_x is related to the minimum value B_m of

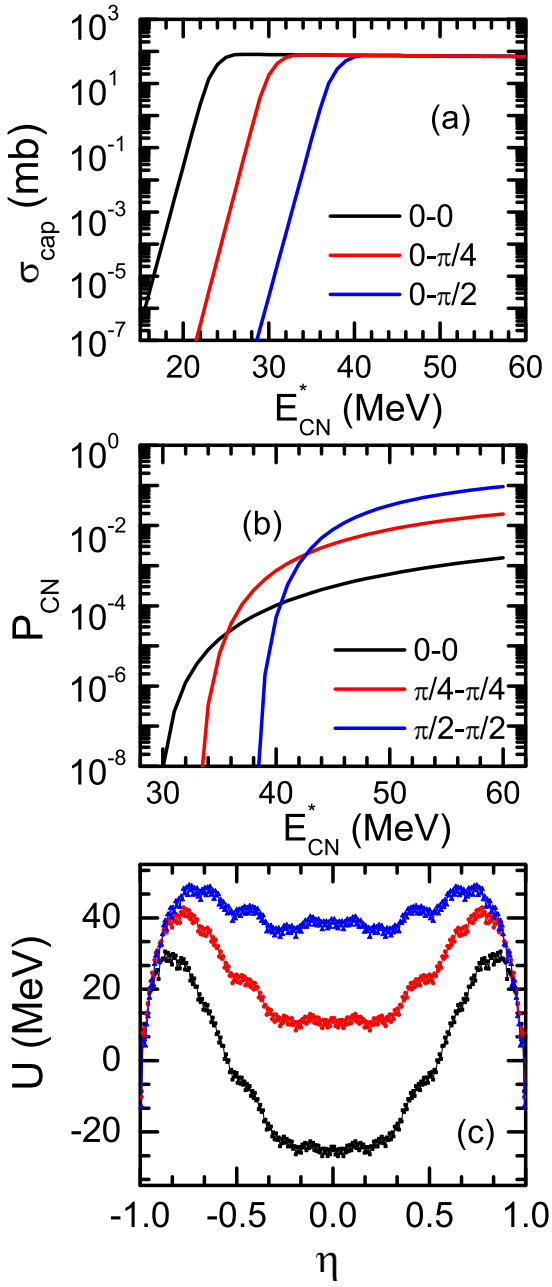

FIG. 2. (a) The capture cross sections for $\theta_2 = 0,\ \pi/4$, and $\pi/2$ are denoted by black, red, and blue solid lines, respectively. (b) The fusion probabilities depend on excitation energies for different orientation angle combinations of projectilelike and targetlike (θ_1, θ_2). (c) The driving potential of DNS as a function of the mass asymmetry η at different orientations.

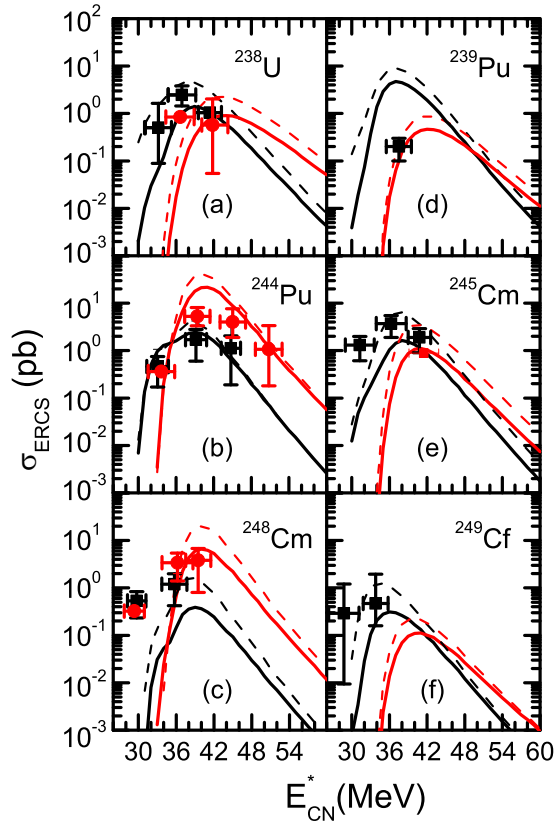

FIG. 3. The calculated results without and with the temperature effects are denoted by dashed and solid lines, respectively. The measured ERCSs [49] of the $3n$ and $4n$ channels are denoted by black solid squares and red solid circles, respectively.

the interaction potential of the nucleus-nucleus. At the same bombarding energy $E_{\rm c.m.}$, the dissipation of energy into the DNS is larger for the lower B_m, which leads to a maximum value of the local excitation energy for the tip-tip case.

In the DNS model, a valence space $\Delta\varepsilon_k = \sqrt{\frac{4\varepsilon_k}{g_k}}$ is formed due to the excitation. Here, it is assumed that the sharing of the local excitation energy between the targetlike and the projectilelike fragments are proportional to their masses $\varepsilon_k = \varepsilon\frac{A_k}{A}$ $(k = 1, 2)$. According to the definition of $\Delta\varepsilon_k$ and ε_k, the most probable mass arrangement should occur when valence space in the DNS is largest, which corresponds to a maximum of the local excitation energy. As displayed in Fig. 2(b), in the lower excitation energy region $E^*_{CN} < 35$ MeV and in the tip-tip case gives the highest fusion probability. For the side-side case, the highest potential-energy surface in the symmetric region is not in favor of quasifission, and the lowest inner fusion barrier that it enhances is fusion. The fusion probability is determined by the local excitation energy and inner fusion barrier together. Therefore, the deviation of the fusion probability for tip-tip and side-side cases decreases with the increase in the excitation energy and then increases with the increase in the excitation energy, up to about two orders of magnitude and tend to be unchanged.

To illustrate the influence of the excitation energy dependence of the potential-energy surface on the fusion process, the excitation functions of the ERCSs for reactions by ^{48}Ca bombarding actinide nuclei to produce elements $Z =$ 112, 114, 116, and 118 are shown in Fig. 3. It is found that the included effect of the excitation energy in the potential-energy surface reduces the fusion probability eventually influencing the production cross section of the SHN. I would like to point out that some data points in Fig. 3 are not supported by the solid lines. However, more data are supported by the

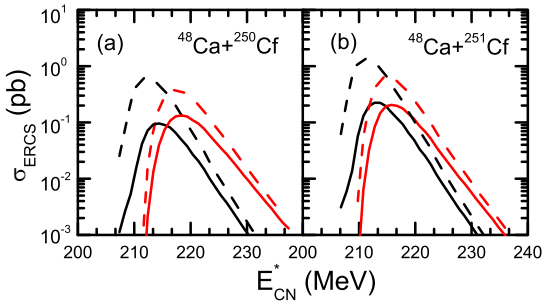

FIG. 4. The ERCSs of yet undiscovered superheavy nuclei $Z = 118$ predicted by considering the dynamical nuclear deformation in the DNS model by the solid lines. The dashed lines show those only considering the nuclear ground-state deformation.

solid lines, which reveal the necessity of considering the excitation energy dependence of the potential-energy surface in the fusion process. The disagreement reveals the defect of my model, which I have to check and further improve.

The maximal $\sigma_{\rm ERCS}$ for SHN with ^{238}U(^{48}Ca, xn)$^{286-xn}$Cn, ^{239}Pu(^{48}Ca, xn)$^{287-xn}$Fl, ^{245}Cm (^{48}Ca, xn)$^{293-xn}$Lv, and ^{249}Cf(^{48}Ca, xn)$^{297-xn}$Og is found in the $3n$-emission channel, and for those with ^{244}Pu(^{48}Ca, xn)$^{292-x}$Fl and ^{248}Cm(^{48}Ca, xn)$^{296-x}$Lv, the $4n$ evaporation-residue channel is more favorable. The results are well in coincidence with the experimental data. The maximal $\sigma_{\rm ERCS}$ appearing in the $3n$ or in the $4n$ channel is determined by the behavior of fusion probability P_{CN} and survival probability $W_{\rm sur}$ with increasing excitation energy. The fusion probability increases with increasing excitation energy, whereas the survival probability for each neutron emission channel increases with increasing excitation energy up to a maximum value and then decreases with the excitation energy. Usually, the maximal $W^{3n}_{\rm sur}$ is larger than the maximal $W^{4n}_{\rm sur}$. Therefore, whether the maximal ERCS appears in the $3n$ or in the $4n$ channel depends on the increasing behavior of P_{CN} with the excitation energy. The well-reproduced trend and absolute value of the maximum cross section for the $3n$ and $4n$ channels indicate that the present increasing speed of the fusion probability is properly described compared to the speed of decreasing or increasing survive probability as increasing excitation energies.

Above results give us the confidence to investigate the ERCSs of fusion reactions leading to new isotopes based on systematic calculations. The ^{48}Ca-induced reactions ^{48}Ca + ^{249,250,251}Cf are studied for the synthesis of isotopes of element $Z = 118$. As one can see in Fig. 3(f), the cross section calculated for ^{294}Og and ^{293}Og and the excitation function of the $3n$ evaporation channel are in good agreement with the experimental data [49]. The predicted maximum value of the ERCS for the production ^{293}Og is 0.112 pb at $E_{\rm c.m.} \approx 219$ MeV. The ERCSs for the $3n$ and $4n$ channels in the ^{48}Ca + ^{250}Cf reaction leading to the formation of ^{295}Og and ^{294}Og isotopes are evaluated, and the excitation functions of the ERCSs are shown in Fig. 4(a). The maximum ERCSs in the $3n$ and $4n$ evaporation channels are 0.096 ($E_{\rm c.m.} \approx 214$ MeV) and 0.127 ($E_{\rm c.m.} \approx 220$ MeV) pb, respectively. The excitation function of the ERCS for the ^{251}Cf(^{48}Ca, xn)$^{299-xn}$Og reaction are shown in Fig. 4(b), and, for the $3n$, $4n$ channels, they are 0.223 ($E_{\rm c.m.} \approx 212$ MeV) and 0.196 ($E_{\rm c.m.} \approx 217$ MeV) pb, respectively. The above ERCSs are close to the present experimental technique limit for the identification of the evaporation residual nuclei.

I have investigated some aspects of the synthesis mechanism of SHN. One finds that: (i) The ERCSs of the$3n$ and $4n$ channels are mainly contributed from the side-side collision ($\pi/2, \pi/2$). The conclusion is consistent with the experimental results in Refs. [20,21]. (ii) The well-reproduced trend and absolute value of the maximum cross section for the $3n$ and $4n$ channels indicates that the present increasing speed of fusion probability is properly described comparing to the speed of changing survive probability as increasing excitation energies. (iii) The predicted ERCSs for ^{293,295,296}Og are close to the present experimental technique limit.

The work was supported by the National Natural Science Foundation of China (Grant No. 11705055), the Hunan Provincial Natural Science Foundation of China (Grant No. 2018JJ3324), and excellent youth fund of the Hunan Provincial Education Department (Grant No. 17B154).

[1] S. Hofmann and G. Münzenberg, Rev. Mod. Phys. **72**, 733 (2000).
[2] S. A. Giuliani, Z. Matheson, W. Nazarewicz, E. Olsen, P.-G. Reinhard, J. Sadhukhan, B. Schuetrumpf, N. Schunck, and P. Schwerdtfeger, Rev. Mod. Phys. **91**, 011001 (2019).
[3] W. J. Swiatecki, Nucl. Phys. A **376**, 275 (1982).
[4] N. Antonenko, E. Cherepanov, A. Nasirov, V. Permjakov, and V. Volkov, Phys. Lett. B **319**, 425 (1993).
[5] V. Y. Denisov and S. Hofmann, Phys. Rev. C **61**, 034606 (2000).
[6] L. Zhu, W. J. Xie, and F. S. Zhang, Phys. Rev. C **89**, 024615 (2014).
[7] V. I. Zagrebaev and W. Greiner, Nucl. Phys. A **944**, 257 (2015).
[8] K. Siwek-Wilczyńska, T. Cap, M. Kowal, A. Sobiczewski, and J. Wilczyński, Phys. Rev. C **86**, 014611 (2012).
[9] X. J. Bao, Y. Gao, J. Q. Li, and H. F. Zhang, Phys. Rev. C **91**, 011603(R) (2015).
[10] W. J. Swiatecki, Prog. Part. Nucl. Phys. **4**, 383 (1980).
[11] G. G. Adamian *et al.*, Nucl. Phys. A **627**, 361 (1997).
[12] A. Diaz-Torres, G. G. Adamian, N. V. Antonenko, and W. Scheid, Phys. Lett. B **481**, 228 (2000).
[13] Y. Aritomo, T. Wada, M. Ohta, and Y. Abe, Phys. Rev. C **59**, 796 (1999).
[14] T. Cap, K. Siwek-Wilczyńska, M. Kowal, and J. Wilczyński, Phys. Rev. C **88**, 037603 (2013).
[15] G. Mandaglio, G. Giardina, A. K. Nasirov, and A. Sobiczewski, Phys. Rev. C **86**, 064607 (2012).

[16] V. Y. Denisov and W. Nörenberg, Eur. Phys. J. A **15**, 375 (2002).
[17] A. Nasirov, A. Fukushima, Y. Toyoshima, Y. Aritomo, A. Muminov, S. Kalandarov, and R. Utamuratov, Nucl. Phys. A **759**, 342 (2005).
[18] V. Zagrebaev and W. Greiner, Phys. Rev. Lett **101**, 122701 (2008).
[19] N. T. Brewer, V. K. Utyonkov, K. P. Rykaczewski, Yu. Ts. Oganessian, F. Sh. Abdullin, R. A. Boll, D. J. Dean, S. N. Dmitriev, J. G. Ezold, L. K. Felker *et al.*, Phys. Rev. C **98**, 024317 (2018).
[20] D. J. Hinde, M. Dasgupta, J. R. Leigh, J. P. Lestone, J. C. Mein, C. R. Morton, J. O. Newton, and H. Timmers, Phys. Rev. Lett **74**, 1295 (1995).
[21] A. Wakhle, C. Simenel, D. J. Hinde, M. Dasgupta, M. Evers, D. H. Luong, R. du Rietz, and E. Williams, Phys. Rev. Lett **113**, 182502 (2014).
[22] Ş. Mişicu and W. Greiner, Phys. Rev. C **66**, 044606 (2002).
[23] L. G. Moretto and R. Stella, Phys. Lett. B **32**, 558 (1970).
[24] A. S. Jensen and J. Damgaard, Nucl. Phys. A **210**, 282 (1973).
[25] I. I. Gontchar, P. Fröbrich, and N. I. Pischasov, Phys. Rev. C **47**, 2228 (1993).
[26] J. Randrup and P. Möller, Phys. Rev. C **88**, 064606 (2013).
[27] Y. Aritomo, Nucl. Phys. A **780**, 222 (2006).
[28] P. Frobrich, Nucl. Phys. A **787**, 170c (2007).
[29] C. C. Sahm, H. G. Clerc, K.-H. Schmidt, W. Reisdorf, P. Armbruster, F. P. Hessberger, J. G. Keller, G. Münzenberg, and D. Vermeulen, Nucl. Phys. A **441**, 316 (1985).
[30] C. Y. Wong, Phys. Rev. Lett. **31**, 766 (1973).
[31] G. G. Adamian, N. V. Antonenko, R. V. Jolos, S. P. Ivanova, and O. I. Melnikova, Int. J. Mod. Phys. E **5**, 191 (1996).
[32] X. J. Bao, S. Q. Guo, J. Q. Li, and H. F. Zhang, Phys. Lett. B **785**, 221 (2018).
[33] X. J. Bao, Nucl. Phys. A **986**, 60 (2019).
[34] N. Wang, Z. Y. Liang, M. Liu, and X. Z. Wu, Phys. Rev. C **82**, 044304 (2010).
[35] P. Möller, J. R. Nix, W. D. Myers, and W. J. Swiatecki, At. Data Nucl. Data Tables **59**, 185 (1995).
[36] V. Y. Denisov and I. Y. Sedykh, Eur. Phys. J. A **54**, 231 (2018).
[37] A. V. Ignatyuk, K. K. Istekov, and G. N. Smirenkin, Sov. J. Nucl. Phys. **29**, 450 (1979).
[38] J. A. Sheikh, W. Nazarewicz, and J. C. Pei, Phys. Rev. C **80**, 011302(R) (2009).
[39] J. C. Pei, W. Nazarewicz, J. A. Sheikh, and A .K. Kerman, Phys. Rev. Lett **102**, 192501 (2009); Nucl. Phys. A **834**, 381c (2010).
[40] T. Rauscher, F.-K. Thielemann, and K.-L. Kratz, Phys. Rev. C **56**, 1613 (1997).
[41] V. Y. Denisov and I. Y. Sedykh, Phys. Rev. C **98**, 024601 (2018).
[42] S. Ayik, B. Schuermann, and W. Nörenberg, Z. Phys. A **279**, 145 (1976).
[43] C. Riedel, G. Wolschin, and W. Nörenberg, Z. Phys. A **290**, 47 (1979).
[44] J. D. Jackson, Can J. Phys **34**, 767 (1956).
[45] I. Dostrovsky, Z. Fraenkel, and G. Friedlander, Phys. Rev **116**, 683 (1959).
[46] X. J. Bao, Chin. Phys. C **43**, 054105 (2019).
[47] N. Bohr and J. A. Wheeler, Phys. Rev. **56**, 426 (1939).
[48] E. M. Kozulin, G. N. Knyazheva, I. M. Itkis, M. G. Itkis, A. A. Bogachev, E. V. Chernysheva, L. Krupa, F. Hanappe, O. Dorvaux, L. Stuttgé *et al.*, Phys. Rev. C **90**, 054608 (2014).
[49] Yu. Ts. Oganessian, V. K. Utyonkov, Yu. V. Lobanov, F. Sh. Abdullin, A. N. Polyakov, I. V. Shirokovsky, Yu. S. Tsyganov, G. G. Gulbekian, S. L. Bogomolov, B. N. Gikal *et al.*, Phys. Rev. C **70**, 064609 (2004); Yu. Ts. Oganessian, V. K. Utyonkov, Yu. V. Lobanov, F. Sh. Abdullin, A. N. Polyakov, R. N. Sagaidak, I. V. Shirokovsky, Yu. S. Tsyganov, A. A. Voinov, G. G. Gulbekian *et al.*, *ibid.* **76**, 011601(R) (2007); Yu. Ts. Oganessian, V. K. Utyonkov, Yu. V. Lobanov, F. Sh. Abdullin, A. N. Polyakov, I. V. Shirokovsky, Yu. S. Tsyganov, G. G. Gulbekian, S. L. Bogomolov, B. N. Gikal *et al.*, *ibid.* **69**, 054607 (2004); Yu. Ts. Oganessian, F. Sh. Abdullin, S. N. Dmitriev, J. M. Gostic, J. H. Hamilton, R. A. Henderson, M. G. Itkis, K. J. Moody, A. N. Polyakov, A. V. Ramayya *et al.*, *ibid.* **87**, 014302 (2013); Yu. Ts. Oganessian, V. K. Utyonkov, Yu. V. Lobanov, F. Sh. Abdullin, A. N. Polyakov, R. N. Sagaidak, I. V. Shirokovsky, Yu. S. Tsyganov, A. A. Voinov, G. G. Gulbekian *et al.*, *ibid.* **74**, 044602 (2006).